Isoscalar transition rates from inelastic alpha scattering

R. Neu and F. Hoyler
Physikalisches Institut der Universität Tübingen, D 7400 Tübingen, Federal Republic of Germany
(Received 27 January 1992)

Isoscalar transition probabilities [$B(IS\lambda)$] have been obtained from the analysis of inelastic α scattering using double-folded optical α-nucleus potentials. The reliability of the proposed method was tested by applying it to three nuclei representing limiting cases of nuclear structure models. Data on ^{208}Pb have been analyzed at $E_\alpha = 23.5$, 79.1, 104, and 139 MeV using the hydrodynamical model. For ^{168}Er ($E_\alpha = 36$ MeV) the model of the asymmetric rotor and for ^{108}Pd ($E_\alpha = 30.5$ MeV) the model of the harmonic vibrator was considered. Excellent agreement of the extracted $B(IS\lambda)$ values with the corresponding $B(E\lambda)$ values (obtained from electromagnetic probes) has been reached. The result of a lifetime measurement for the two-quadrupole-phonon 4^+ state at 2055 keV in ^{168}Er has been confirmed.

PACS number(s): 23.20.Js, 25.55.Ci, 24.10.Eq

I. INTRODUCTION

A crucial test of the theoretical understanding of collective low-lying nuclear excitations is whether the deexcitation of these levels can be predicted correctly by the model in question. Since low-lying states are considered, one needs the experimental knowledge of the reduced electromagnetic $B(E\lambda)$ or $B(M\lambda)$ values and therefore one is normally restricted to multipoles with $\lambda \leq 2$. On the other hand, most nuclear models have to incorporate higher multipoles (octupole, hexadecapole, etc.) to successfully describe even the lowest excited states in a nucleus.

The use of inelastic scattering of hadronic probes to gain information on surface vibrations or permanent deformation of the nuclear shape has a long history (see, e.g., Bernstein [1]). Especially the analysis of inelastic α scattering has widely been used to extract this information, since the strong absorption of α particles in nuclear matter restricts the interaction to the surface and thus to the region where the effects of surface vibration and nuclear deformation are expected to be strongest. Moreover, the α particle interacts with protons *and* neutrons yielding information on mass transition densities, whereas Coulomb excitation and (e,e') probe only the charge distribution of the nucleus. The high binding energy and the zero spin and isospin of the α particle make the interpretation rather uncomplicated, but restricts the information to isoscalar properties of the nucleus. The Satchler theorem [2] connects the multipole moments of the optical potential to those of the matter distribution. If one assumes that protons and neutrons move in phase with the same amplitude, these moments are also connected to the electromagnetic transition probabilities. The use of the Satchler theorem is only justified if the optical potentials have been obtained from a proper folding procedure.

In a systematic investigation of elastic and inelastic α scattering on *p*- and *sd*-shell nuclei [3–6] it has been shown that the use of double-folded optical potentials in optical model as well as in coupled channel calculations describes the experimental data very well. These potentials are calculated from mass densities deduced from experimental charge distributions [7] and a density-dependent M3Y effective nucleon-nucleon interaction [8].

From the deformation parameters of these deformed optical potentials we calculated isoscalar transition strength values which compare favorably with the results from electromagnetic probes. In contrast to many investigations, which use a Woods-Saxon parametrization of the optical potential, these folded potentials are appropriate to the use of the Satchler theorem.

The success of these calculations motivated the present investigation which applies this method to the heavy double magic nucleus ^{208}Pb, the deformed rare-earth nucleus ^{168}Er, and the spherical nucleus ^{108}Pd. Our main aim is to show that the consistent treatment of the analysis of inelastic α scattering allows us to extract reliable isoscalar transition probabilities not only for transitions, which can be compared to the values obtained from electromagnetic probes, but also for higher multipole transitions not accessible by other methods.

Many experimental and theoretical investigations have been devoted to the elastic scattering of α particles on ^{208}Pb and to the inelastic scattering to the first excited collective 3^- state at 2.6 MeV in this isotope [9–12]. We include a reanalysis of these data to demonstrate the success of our method in the description of both the elastic scattering and the inelastic excitation of this highly collective octupole vibrational state. It is beyond the scope of the present contribution to discuss the subtle differences of the proton and neutron mass and transition densities, which could be extracted on the basis of the extensive data sets at $E_\alpha = 104$ (Ref. [11]) and 139 MeV (Ref. [12]) bombarding energy.

The level scheme and the transition probabilities of the $0^+, 2^+, 4^+$ triplet in ^{108}Pd exhibit the features of an almost unperturbed harmonic vibrator. The extensive data set on elastic and inelastic scattering of α particle on this nucleus of Riech *et al.* [13] allows a detailed test of our method for spherical nuclei.

Besides the fact that ^{168}Er is one of the most extensive-

ly studied deformed nuclei, the reanalysis of the ^{168}Er data of Govil *et al.* [14] was further motivated by a recent measurement of the lifetime of the $4^+_{\gamma\gamma}$ level at 2055 keV in this nucleus [15]. The ratio $R(4^+_{\gamma\gamma}) = B(E2,4^+_{\gamma\gamma}\rightarrow 2^+_\gamma)/B(E2,2^+_\gamma\rightarrow 0^+_{\text{g.s.}})$ obtained from the lifetimes of the $4^+_{\gamma\gamma}$ and 2^+_γ levels is quoted to be $0.52 < R(4^+_{\gamma\gamma}) < 1.61$ and established the existence of a two-phonon $K^\pi = 4^+$ gamma vibration in ^{168}Er. This state is also observed in the spectra of inelastic α scattering of Ref. [14], and was included in our analysis to test whether the $R(4^+_{\gamma\gamma})$ value of Ref. [15] can be reproduced. We also want to contribute new information on the hexadecapole degree of freedom, which plays an important role in some theoretical descriptions as, for example, the *sdg*-interacting boson model [16].

In Sec. II we will outline the methods used to analyze the experimental data of inelastic α scattering using a double-folded α-nucleus optical potential on spherical and on deformed nuclei. In Sec. III the results of the coupled channel calculations will be presented and the deduced isoscalar transition rates will be compared to data obtained from electromagnetic probes. These results will be summarized in Sec. IV which also concludes this investigation.

II. COUPLED CHANNEL ANALYSIS

A. Double-folded optical potential

The calculations of the optical potentials were carried out in the framework of the double-folding model. The real part of the optical potential is described by

$$U_F(\mathbf{r}) = \lambda_F \int d\mathbf{r}_1 \int d\mathbf{r}_2 \rho_T(\mathbf{r}_1)\rho_\alpha(\mathbf{r}_2) \times t(E,\rho_T,\rho_\alpha,\mathbf{s}=\mathbf{r}+\mathbf{r}_2-\mathbf{r}_1) , \quad (1)$$

where $\mathbf{r}$ is the separation of the centers of mass of the colliding target nucleus and the α particle, $\rho_T(\mathbf{r}_1)$ and $\rho_\alpha(\mathbf{r}_2)$ are the respective nucleon densities, and λ_f is an overall normalization factor. For the effective interaction t the density-dependent form of the M3Y nucleon-nucleon interaction [8] has been chosen. For the density distribution of the target nucleus ρ_T we used the experimental charge distribution [7] obtained from electron scattering and unfolded from the finite charge distribution of the proton. Since to our knowledge no information about the neutron distributions is available for the nuclei ^{108}Pd and ^{168}Er, it is assumed to be N/Z times the proton distribution. In the case of the nucleus ^{208}Pb, a neutron distribution from shell-model calculations [17] is added to the experimental charge distribution. For the density distribution of the α particle a Gaussian form was used [18]. Details of the numerical computation of the potential $U_F(\mathbf{r})$ are described in Ref. [3]. In the coupled channel calculations within the rotor model the α-nucleus interaction is described by a deformed optical potential $V(r,R)$. In order to gain a properly deformed folding potential, in a first step the potential calculated by the double-folding procedure is expanded in a Fourier-Bessel series of 20 terms:

$$V(r,R_{\text{FB}}) = \sum_{\nu=1}^{20} \alpha_\nu j_0\left[\frac{\nu\pi r}{R_{\text{FB}}}\right] , \quad (2)$$

with a cutoff radius $R_{\text{FB}} = 12$ fm.

Subsequently, in the second step, an angular dependence of the cutoff radius R_{FB} is introduced as will be outlined in Sec. II B 2. The radial dependence of the imaginary potential was taken as a sum of a Woods-Saxon volume and surface term. This parametrization turned out to be more successful than the use of a Fourier-Bessel series with the same number of adjustable parameters. In all calculations the Coulomb potential is deformed in the usual way [19].

B. The coupled channel formalism

Following Tamura [19] the coupling matrix elements can be expressed in the general form

$$\langle lI|V_{cp}|l'I'\rangle = \sum_\lambda \sum_\kappa v_{\lambda\kappa}(r)\langle \Psi_I\|Q^{(\kappa)}_\lambda\|\Psi_{I'}\rangle A(lI,l'I',\lambda J) . \quad (3)$$

The factors $A(lI,l'I',\lambda J)$ are purely geometric and model independent. In contrast, the other two factors, namely, the radial form factor $v_{\lambda\kappa}(r)$ and the reduced matrix elements $\langle \Psi_I\|Q^{(\kappa)}_\lambda\|\Psi_{I'}\rangle$, are model dependent.

1. *The vibrational and the hydrodynamical model*

The vibrational model (HVM) describes the dynamical deformation of the spherical surface of the nucleus by the parametrization:

$$R(\vartheta,\varphi) = R_0\left[1+\sum_{\lambda\kappa}\alpha_{\lambda\kappa}Y_{\lambda\kappa}(\Omega)\right] . \quad (4)$$

By expanding the potential in powers of $Y_{\lambda\kappa}(\Omega)$ around the equilibrium radius R_0 to first order, we obtain

$$V(r-R) = V(r-R_0) + \sum_{\lambda\kappa} R_0 \frac{dV}{dr}(r-R_0)\alpha_{\lambda\kappa}Y_{\lambda\kappa}(\Omega) = V_{\text{diag}} + V_{\text{cp}} . \quad (5)$$

Generally, the coupling potential V_{cp} can be expressed as

$$V_{\text{cp}} = \sum_{\lambda\kappa} v_{\lambda\kappa}(r) Q_{\lambda\kappa} Y_{\lambda\kappa}(\Omega) . \quad (6)$$

Thus, the radial form factor is given as

$$v_{\lambda\kappa}(r) = R_0 \frac{dV}{dr}(r-R_0) . \quad (7)$$

In the case of the hydrodynamical model (HDM) of Tassie [20] instead of this radial dependence we have

$$v_{\lambda\kappa}(r) = r\left[\frac{r}{R_0}\right]^{\lambda-2}\frac{dV}{dr}(r) . \quad (8)$$

The transition operator $Q_{\lambda\kappa} = \alpha_{\lambda\kappa}$ can be decomposed in the usual way into operators $b_{\lambda\kappa}$ and $b^*_{\lambda\kappa}$ which annihilate and create a phonon of vibration:

$$\alpha_{\lambda\kappa}=\frac{\beta_\lambda}{\sqrt{2\lambda+1}}[b_{\lambda\kappa}+(-1)^\kappa b^*_{\lambda-\kappa}] \ . \tag{9}$$

Using these $b^*_{\lambda\kappa}$ and denoting the ground state by $|0\rangle$, a one-phonon state with spin λ and its projection κ can be written as

$$|1;\Psi_{\lambda\kappa}\rangle=b^*_{\lambda\kappa}|0\rangle \ . \tag{10}$$

The root mean square deformation parameter β_λ is defined in such a way that β^2_λ stands for the expectation value of $\sum_\kappa|\alpha_{\lambda\kappa}|^2$ in the nuclear ground state:

$$\beta^2_\lambda=\langle 0|\sum_\kappa|\alpha_{\lambda\kappa}|^2|0\rangle \ . \tag{11}$$

Using these dynamical deformation operators for the wave functions, the results for those reduced matrix elements which were used in this work are summarized as follows.

For the transition with the multipolarity λ from the ground state to a one-phonon state we get

$$\langle 1;\Psi_I\|Q_\lambda\|0;0\rangle=\delta_{\lambda I}(-1)^I\beta_\lambda \ . \tag{12}$$

In the case of the transition from a one-quadrupole-phonon state to a two-quadrupole-phonon state the reduced matrix elements are given by

$$\langle 2;\Psi_I\|Q_2\|1;\Psi_2\rangle=\beta_2\left[\frac{2(2I+1)}{5}\right]^{1/2} \ . \tag{13}$$

In order to simulate anharmonicities, a mixing between two-phonon amplitudes and one-phonon amplitudes can be assumed in the construction of the triplet $(I=0^+,2^+,4^+)$ states [21]:

$$|\Psi_I\rangle_{\text{triplet}}=\cos\varphi_I|1;\Psi'_I\rangle+\sin\varphi_I|2;\Psi''_I\rangle \ . \tag{14}$$

The mixing allows a direct transition from the ground state to each of the triplet states. The matrix elements (12), (13) now have to be multiplied by $\cos\varphi_I$ in the case of a one-phonon transition to the triplet state and by $\sin\varphi_I$ in the case of a two-phonon transition.

2. *The extended asymmetric rotational model*

In this section the same notation as in our previous work [4] on ^{24}Mg will be used. In the asymmetric rotor model (ARM) the shape of the nucleus is given in the body-fixed system by expanding the radius parameter R_{FB} up to $\lambda=8$:

$$R_{\text{FB}}(\Omega')=R_{\text{FB0}}\left\{1+a_{20}Y_{20}(\Omega')+\frac{1}{\sqrt{2}}a_{22}[Y_{22}(\Omega')+Y_{2-2}(\Omega')]+a_{40}Y_{40}(\Omega')+\frac{1}{\sqrt{2}}a_{42}[Y_{42}(\Omega')+Y_{4-2}(\Omega')]\right.$$
$$\left.+\frac{1}{\sqrt{2}}a_{44}[Y_{44}(\Omega')+Y_{4-4}(\Omega')]+a_{60}Y_{60}(\Omega')+\frac{1}{\sqrt{2}}a_{62}[Y_{62}(\Omega')+Y_{6-2}(\Omega')]+a_{80}Y_{80}(\Omega')\right\} , \tag{15}$$

where the $a_{\lambda\kappa}$ are parametrized as follows:

$$a_{20}=\beta_2\cos\gamma_1, \quad a_{40}=\beta_4\cos\gamma_2, \quad a_{22}=\beta_2\sin\gamma_1, \quad a_{42}=\beta_4\sin\gamma_2\cos\gamma_3, \quad a_{44}=\beta_4\sin\gamma_2\sin\gamma_3 \ , \tag{16a}$$

and

$$a_{60}=\beta_6\cos\gamma_4, \quad a_{62}=\beta_6\sin\gamma_4, \quad a_8=\beta_8 \ . \tag{16b}$$

In an extension of the well known model of Davydov and Filippov [22] the moments of inertia up to $\lambda=4$ are given by Baker *et al.* [23]. The rotational Hamiltonian H_{rot} can be expressed in terms of the moments of inertia of the deformed nucleus [24]. The nuclear wave function Ψ^n_{IM} of the nth rotational state with spin I may be written as a superposition of the eigenfunctions of the symmetric rotor Φ_{IMK}

$$\Psi^n_{IM}=\sum_{K=0,2,4}A^n_{IK}\Phi_{IMK} \ , \tag{17}$$

with

$$\Phi_{IMK}(\varepsilon_i)=\left[\frac{2I+1}{16\pi^2(1+\delta_{K0})}\right]^{1/2}[D^I_{MK}(\varepsilon_i)+(-1)^I D^I_{M-K}(\varepsilon_i)] \ , \tag{18}$$

where $D^I_{MK}(\varepsilon_i)$ are the Wigner rotation matrices and ε_i the Euler angles. Through the diagonalization of the collective Hamiltonian H_{rot} in the Φ_{IMK} basis, the energies of the states and the band mixing coefficients A^n_{IK} are obtained [24]. In order to solve the coupled equations we have to calculate the coupling matrix elements

$$\langle lI_n|V_{\text{cp}}|l'I'_{n'}\rangle:=\langle(Y_{l_n}\times\Psi^n_I)_{JM_l}|V_{\text{cp}}|(Y_{l'_{n'}}\times\Psi^{n'}_{I'})_{JM_l}\rangle$$
$$=\sum_{K=0,2,4}\sum_{K'=0,2,4}A^n_{IK}A^{n'}_{I'K'}\langle(Y_{l_n}\times\Phi_{I_nK})_{JM_l}|V_{\text{cp}}|(Y_{l'_{n'}}\times\Phi_{I'_{n'}K'})_{JM_l}\rangle \ , \tag{19}$$

with

$$(Y_l \times \Phi_{IK})_{JM_l} = \sum_{mM} i^l (lImM|JM_l) Y_{lm}(\Omega) \Phi_{IMK} \ , \tag{20}$$

where A^n_{IK} are the band-mixing coefficients of the wave functions of the actual nth state with spin I, and Φ_{IMK} are the eigenfunctions of the symmetric rotor given in Eq. (18). The coupling potentials $V_{\rm cp}$ are derived from the Legendre expansion of the deformed interaction potential $V(r,R(\Omega'))$ transformed from the body-fixed to the space-fixed system:

$$V(r,R(\Omega)) = V_{\rm diag} + V_{\rm cp} \ , \tag{21}$$

$$V_{\rm cp} = \sum_{\substack{\lambda,\mu(\lambda\neq 0) \\ \kappa=0,2,4}} v_{\lambda\kappa}(r) \left[\frac{1}{\sqrt{2}} [D^\lambda_{\mu\kappa}(\varepsilon_i) + D^\lambda_{\mu-\kappa}(\varepsilon_i)] \right] Y_{\lambda\mu}(\Omega) \ , \tag{22}$$

with Ω' referring to the body-fixed and Ω to the space-fixed system.

The radial shape of the transition potential within the ARM is given by the radial form factor $v_{\lambda\kappa}(r)$

$$v_{\lambda\kappa}(r) = \frac{i^\lambda}{1+\delta_{\kappa 0}} \int V(r,R(\Omega'))[Y_{\lambda\kappa}(\Omega') + Y^*_{\lambda\kappa}(\Omega')] d\Omega' \tag{23}$$

with $\lambda = 2,4,6,8$ and $\kappa = 0,2,4$. Comparing Eq. (22) with the general ansatz for the coupling potential $V_{\rm cp}$ given in Eq. (6) we can see that the transition operators $Q^{(\kappa)}_\lambda$ are just the rotation matrices:

$$Q^{(\kappa)}_\lambda = \frac{1}{\sqrt{2}} (D^\lambda_{;\kappa} + D^\lambda_{;-\kappa}) \ . \tag{24}$$

The reduced matrix elements of the transition operator (24) with respect to the target states (17) are therefore given as

$$\langle \Psi^n_I \| Q^{(\kappa)}_\lambda \| \Psi^{n'}_{I'} \rangle = \sum_{K=0,2,4} \sum_{K'=0,2,4} A^n_{IK} A^{n'}_{I'K'} \langle \Phi_{IK} \| \frac{1}{\sqrt{2}} (D^\lambda_{;\kappa} + D^\lambda_{;-\kappa}) \| \Phi_{I'K'} \rangle \ . \tag{25}$$

C. Isoscalar transition rates and quadrupole moments

For a given mass distribution $\rho(\mathbf{r})$ the normalized multipole moments are given in the body-fixed system as

$$q_{\lambda\kappa} := \frac{1}{1+\delta_{\kappa 0}} \int \rho(\mathbf{r}) r^\lambda [Y_{\lambda\kappa}(\Omega') + Y^*_{\lambda\kappa}(\Omega')] d\mathbf{r} \ ,$$

with

$$\int \rho(\mathbf{r}) d\mathbf{r} = 1 \ . \tag{26}$$

Expanding $\rho(\mathbf{r})$ in spherical harmonics

$$\rho(\mathbf{r}) = \sum_{lm} \rho_{lm}(r) Y_{lm}(\Omega') \tag{27}$$

yields

$$q_{\lambda\kappa} = \int r^{\lambda+2} \rho_{\lambda\kappa}(r) dr \ . \tag{28}$$

According to the theorem of Satchler [2,25,26] the normalized mass distribution can be replaced by the normalized potential, if the real part V_R of the effective scattering potential can be described by a folding ansatz with a density-independent effective NN interaction (implicit folding procedure). In this case we get

$$q_{\lambda\kappa} = \frac{\int v_{\lambda\kappa}(r) r^{\lambda+2} dr}{J_R} \ , \tag{29}$$

with the volume integral J_R and with $v_{\lambda\kappa}(r)$ given in Eqs. (7), (8), or (23). In the case of the static deformation the integral in Eq. (29) has to be calculated numerically. In the case of the HVM or HDM the deformation is dynamical and symmetrical, therefore the calculation of $v_{\lambda\kappa}$ is independent of the angles and of κ. By partial integration, using Eq. (7), Eq. (29) reduces to

$$q_{\lambda 0} = \frac{R_0(\lambda+2) \int V(r) r^{(\lambda+1)} dr}{J_R} \ . \tag{30}$$

In the case of the hydrodynamical model we get in an analogous way

$$q_{\lambda 0} = \frac{R_0^{2-\lambda}(2\lambda+1) \int V(r) r^{2\lambda} dr}{J_R} \ . \tag{31}$$

In reality the effective NN interaction is density dependent and Eq. (28) has to be corrected accordingly. Within the method of implicit folding these corrections have been calculated [27,28] to be in the order of a few percent for quadrupole excitations. Recent explicit folding calculations [29,30] for inelastic α scattering accounting also for dynamic density dependence give even smaller corrections. Therefore we used Eq. (29) without any corrections for the density dependence.

The isoscalar moments $m_{IS\lambda\kappa}$ can be expressed then by the normalized potential moments $q_{\lambda\kappa}$ multiplied by the nuclear charge Ze for easy comparison to the electromagnetic moments:

$$m_{IS\lambda\kappa} := Z e q_{\lambda\kappa} \ . \tag{32}$$

By multiplying $IS\lambda$ moments with the reduced $IS\lambda$ matrix elements for a transition $I' \rightarrow I$ we get

$$M_{IS\lambda}(I'-I) = \sum_\kappa m_{IS\lambda\kappa} \langle \Psi^n_I \| Q^{(\kappa)}_\lambda \| \Psi^{n'}_{I'} \rangle \ , \tag{33}$$

where in the case of the HVM and the HDM the sum reduces to one term, and n denotes again the number of

the state with spin I. The $IS\lambda$ isoscalar transition probability is then given by the $B(IS\lambda)$ value as

$$B(IS\lambda,I'\rightarrow I)=(2I'+1)^{-1}M^2_{IS\lambda}(I'\rightarrow I)\ . \tag{34}$$

Furthermore, the diagonal $IS2$ matrix elements from the ARM are related to the spectroscopic quadrupole moments of the excited states by

$$eQ_I=\left[\frac{16\pi}{5}\frac{I(2I-1)}{(I+1)(2I+1)(2I+3)}\right]^{1/2}M_{IS2}(I\rightarrow I)\ . \tag{35}$$

III. RESULTS

All calculations have been performed using a modified version of the coupled channel code ECIS [31]. The shape of the real part of the optical potential was determined from the folding procedure and the deformation parameters as outlined in Sec. II. Thus besides the deformation parameters only the normalization factor λ_f was allowed to vary during the search. We want to stress the fact that in this way also the shape of the transition densities for the different multipolarities is fixed. For the imaginary part of the potential and the transition form factor the same values for the deformation length as for the real part have been used throughout.

A. The ^{208}Pb(α,α') reaction

The first excited 3^- state at an excitation energy of 2.6 MeV in ^{208}Pb is maybe the best example of a collective octupole vibration, and has prompted many experimental and theoretical investigations. It is thus an ideal case to study the validity of the proposed method to extract information on isoscalar transition strengths.

Detailed experimental investigations of the elastic and inelastic scattering of α particles on ^{208}Pb have been reported by Lilley *et al.* [9] at 23.5 MeV, Rutledge and Hiebert [10] at 79.1 MeV, Corcalciuc *et al.* [11] at $E_\alpha=104$ MeV, and Goldberg *et al.* [12] at $E_\alpha=139$ MeV. The data near the Coulomb barrier have been analyzed with special emphasis on Coulomb effects. The data of Rutledge and Hiebert are to our knowledge the only published angular distribution of the first excited 2^+_1 at 4.08 MeV in ^{208}Pb measured over a substantial angular range. The 104 MeV data have been analyzed using a model-independent transition density to investigate possible differences in the proton and neutron strength for this transition.

Kobos *et al.* [8] used the 139 MeV data to test the folding model using a density-dependent force and also investigated differences in the proton and neutron matrix elements in adjusting the proton part to the $B(E3)$ value from electromagnetic probes.

The present analysis of these excellent experimental data does not aim to investigate fine details of the proton or neutron transition density, but is intended to show that isoscalar transition densities obtained from the folding optical potential result in a good description of the elastic and inelastic scattering of α particles of this well-studied collective transition for different energies of the incident particle.

First the data have been analyzed using the standard vibrational transition form factor. For the two lower incident energies very good fits to the data could be obtained. The data at 104 MeV and especially at 139 MeV could not be reproduced as well as the low-energy data. The calculation for the 139 MeV data [dotted line in Fig. 1(d)] overestimates the data points for the 3^- state for angles $\Theta_{\text{c.m.}}>55°$ by a factor of 2, even though it underestimates the experimental results for small scattering angles ($\Theta_{\text{c.m.}}<20°$) by about 20%. Even more striking is the fact that the extracted $B(IS3)$ values are systematically much higher than the values obtained from electromagnetic probes [32], and moreover it was not possible to obtain consistent $B(IS3)$ values for the four energies considered. Using the expression

$$\sqrt{(2L+1)B(EL,L\rightarrow 0)}=\frac{3}{4\pi}\beta_C ZeR^L \tag{36}$$

for the relation of the charge density deformation parameter β_C to the electromagnetic matrix element, one obtains $9.1\times10^4 e^2\,\text{fm}^6$ for the two lower incident energies, which agrees very well with the adopted value of $8.74\times10^4 e^2\,\text{fm}^6$ obtained from (e,e') experiments, whereas the extracted $B(IS3)$ values exceed the adopted value by a factor of approximately 1.7.

Transition potentials obtained from the HDM have already been successfully used by Bertrand *et al.* [33] in the description of giant multipole resonances from inelastic scattering of 152 MeV α particles. In this investigation the transition potential was obtained in folding the charge transition density with a nucleon-α interaction (single folding). In the present work the transition potential is assumed to be of the form given in Eq. (8) as described in Sec. II. As can be seen from Figs. 1(a)–1(d) this prescription results in very good fits for all incident energies. The parameters for the optical potentials (listed in Table I) are similar to those obtained in a detailed investigation of elastic α scattering on ^{208}Pb in the energy range 19–139 MeV (Ref. [34]). They show a smooth energy dependence revealing the expected increase in the volume integral of the imaginary and the decrease in the real part of the optical potential. The shape of the optical potentials is illustrated in Fig. 2 for the four energies investigated and compared to a Woods-Saxon potential (dashed line) obtained by Goldberg *et al.* [12] from a fit to the elastic scattering data at $E_{\text{lab}}=139$ MeV.

It has been pointed out in Sec. II that only for lead a correction for the difference between nuclear mass and charge distribution has been taken into account. Calculations neglecting this correction gave poorer fits to the data, but the resulting $B(IS3)$ value differed by not more than 10% from the best-fit results.

As shown by Lilley *et al.* [9] the data near the Coulomb barrier are sensitive to the deformation of the Coulomb potential. The deep minimum at around $\Theta_{\text{c.m.}}=80°$ for the 23 MeV data is due to a destructive interference between the nuclear and the Coulomb contributions to the transition strength. This is illustrated in

TABLE I. Parameters of the optical potentials for ^{208}Pb ($R_c = 7.11$ fm, $R_0 = 6.3$ fm).

E_α (MeV)	λ_f	W (MeV)	r (fm)	a (fm)	β_3
23.5	1.300	6.77	1.639	0.269	0.0486
79.1	1.356	14.85	1.560	0.602	0.0548
104	1.352	16.53	1.549	0.617	0.0499
139	1.355	19.59	1.480	0.755	0.0546

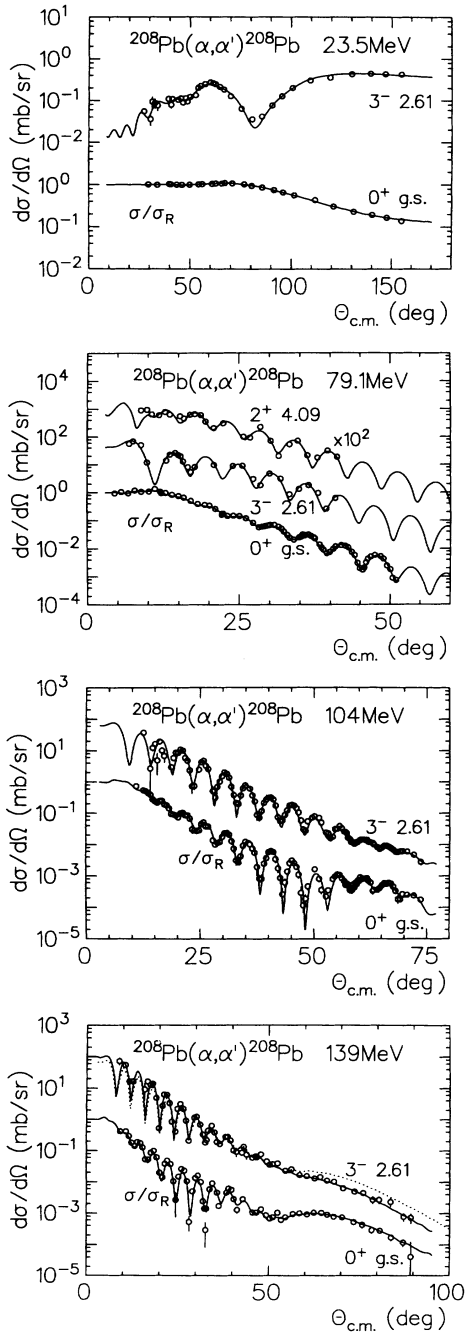

FIG. 1. Inelastic α scattering on ^{208}Pb at (a) 23.5 MeV (Ref. [9]), (b) 79.1 MeV (Ref. [10]), (c) 104 MeV (Ref. [11]), and (d) 139 MeV (Ref. [12]). The solid lines show results of calculations within the HDM. The dotted line in (d) is calculated within the HVM.

Fig. 3 by the dashed ($\beta_3 = 0$) and full ($\beta_C = 0$) lines. This shows the importance of the effects due to Coulomb excitation at very low energies. Using a Woods-Saxon parametrization, Lilley *et al.* [9] had to introduce a different deformation for the two contributions to obtain a good description of the inelastic scattering data. The fits shown in Fig. 1 are all performed in deforming a charged sphere with a reduced radius $r_C = 1.2$ fm, which corresponds to the rms radius of the charge distribution. The deformation parameter $\beta_C = 0.110$ obtained from the fit to the data results in a $B(E3)$ value of $8.6 \times 10^4 e^2\,\mathrm{fm}^6$, which compares very well with the extracted $B(IS3)$ value of $8.0 \times 10^4 e^2\,\mathrm{fm}^6$.

The fit to the 2^+ data at 79 MeV, shown in Fig. 1(b), was performed using the HVM. Here one can also extract a value for the dynamical quadrupole deformation parameter. From the fitted value of $\beta_2 = 0.056$ one obtains a $B(IS2, 2^+ \rightarrow 0^+)$ value of $585 e^2\,\mathrm{fm}^4$ (8 W.u., where W.u. represents Weisskopf unit), which compares very well with the adopted value given in Ref. [35]. The introduction of a rearrangement term $\langle 3^- \| Q_2 \| 3^- \rangle$ did not significantly improve the description of the experimental data. Nevertheless, the fit gave a value for this matrix element from which one obtains a quadrupole moment of approximately 30 fm^2. The absolute value is at variance with the value given in Ref. [36]. The value of the quadrupole moment of the 3^- level is of importance

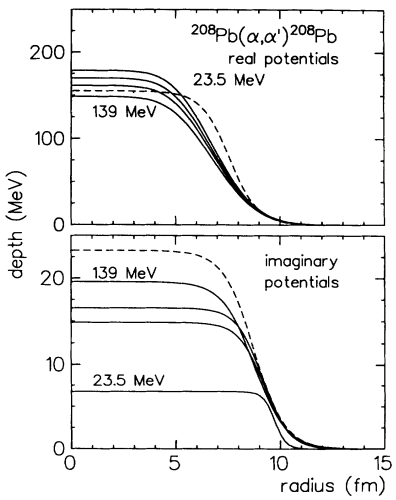

FIG. 2. Real and imaginary potentials used in the analyses (solid lines). The dashed line gives for comparison the Woods-Saxon potential used by Goldberg *et al.* [12].

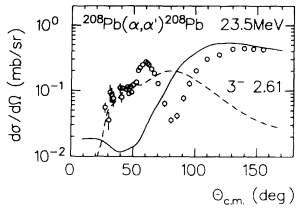

FIG. 3. Decomposition of the excitation of the 3^- state of ^{208}Pb at 23.5 MeV. The solid line shows the result of a pure nuclear excitation ($\beta_c=0$) and the dashed line the result of a pure Coulomb excitation ($\beta_3=0$).

in the prediction of the possible splitting of the spin $(0-6)^+$ two octupole phonon multiplet due to the quadrupole interaction.

The resulting $B(IS3)$ values are also listed in Table II. Using the transition potential from the HDM one obtains consistent values for the reduced isoscalar transition probability for the four incident energies considered, which agree well with the adopted value for the electromagnetic $E3$ transition probability. At the level of precision reached in this work no conclusion on differences in the proton and neutron moments can be made. It should be pointed out that the present investigation has reached an unprecedented degree of agreement between experimental data and calculation.

B. The ^{168}Er(α,α') reaction

We have chosen ^{168}Er to illustrate the reliability of inelastic α scattering for the determination of $B(IS\lambda)$ values for several reasons.

Experimentally Govil *et al.* [14] have measured this reaction with good energy resolution and have identified many states with spin, parity, and rotational band assignment known from other investigations. Especially from thermal neutron capture experiments [37] a complete level scheme for all levels with spin less than $5\hbar$ is known up to an excitation energy of more than 2 MeV.

Recently the measurement [15] of the lifetimes of the $K=4^+$ bandhead at 2055 keV and of the 5^+ member of this band has for the first time evidenced the existence of a collective two-phonon γ-vibrational band as predicted, for example, by the multiphonon model by Piepenbring [38]. The 4^+ bandhead has also been observed in the (α,α') work of Ref. [14] and thus offers a unique possibility to compare our method with the results from lifetime measurements for a two-phonon excitation. The Coulomb excitation measurement of Kotlinsky *et al.* [39] offers further the possibility to compare the results for $B(IS2)$ values from inelastic scattering with the $B(E2)$ values extracted from electromagnetic probes.

The extended asymmetric rotational model as detailed in Sec. II B 2 has been used to analyze the data. After the determination of "reasonable" start values for the deformation parameters obtained in an iterative procedure by building up an increasingly complex coupling scheme a search for best-fit parameters has been carried out using the complete coupling scheme. It turned out that the data are best reproduced with a very low volume integral of the real optical potential (very small λ_f). The extracted transition strength values, however, are almost unaffected by the variation of λ_f, since the moments of the real optical potential are fixed by the folding procedure. To properly account for the Coulomb effects the integration to determine the scattering amplitudes has been extended out to 50 fm. The parameters of the optical potential are listed in Table III; the deformation parameters are given in Table IV. The resulting band-mixing coefficients A^n_{IK} for $I,K\leq 4$ are given in Table V. For the $6^+_{\text{g.s.}}$, 6^+_γ, and the $8^+_{\text{g.s.}}$ states no band mixing is assumed. Table VI gives the integral values of the undeformed potential.

The quality obtained in this fit can be judged from Fig. 4, where the results for the elastic scattering and the excitation of the $2^+_{\text{g.s.}}, 2^+_\gamma, 4^+_{\text{g.s.}}, 4^+_\gamma$, and the $4^+_{\gamma\gamma}$ states are shown together with the experimental data from Ref. [14]. The description of the $6^+_{\text{g.s.}}, 6^+_\gamma$, and the $8^+_{\text{g.s.}}$ states, which is not shown in this work, has reached the same agreement.

The resulting $B(IS\lambda)$ values are listed in Table VII and compared to the results from Coulomb excitation [39]. A good agreement between the two data sets can be observed. In order to compare our transition strengths to the results obtained using a Woods-Saxon parametrization of the optical potential [14] we recalculated the reduced matrix elements also for transitions not quoted by Govil *et al.* The most striking difference is the decrease in hexadecapole strength of almost a factor of 2 in the reduced matrix elements to the $4^+_{\text{g.s.}}$ and the $4^+_{\gamma\gamma}$ state. The $B(IS4)$ value for the 4^+_γ to g.s. transition of $4.46\times10^5 e^2\,\text{fm}^8$ is very similar to the result found in (p,p') (Ref. [40]), but for the transition $4^+_1\rightarrow 0^+_1$ their $B(IS4)$ value is larger by a factor of 30 compared to our value.

From Table VII one reads a value of about 1.5 for the $R(4^+_{\gamma\gamma})$ value defined in the Introduction. This result agrees very well with the result of the lifetime measurement published in Ref. [15] and confirms the collective nature of this bandhead of the first $K^\pi=4^+$ band in ^{168}Er.

TABLE II. Integral values for ^{208}Pb.

E_α (MeV)	$J_R/4A$ (MeV fm^3)	$\langle r_R^2\rangle^{1/2}$ (fm)	$J_I/4A$ (MeV fm^3)	$\langle r_I^2\rangle^{1/2}$ (fm)	$B(IS3,3\rightarrow 0)$ ($10^5 e^2\,\text{fm}^6$)
23.5	343.0	6.28	31.5	7.59	0.80
79.1	323.8	6.28	61.5	7.50	1.02
104	307.9	6.28	67.1	7.47	0.86
139	285.2	6.29	71.4	7.35	1.05

TABLE III. Parameters of the optical potentials for ^{108}Pd and ^{168}Er (^{108}Pd: $R_c=6.665$ fm, $R_0=5.27$ fm; ^{168}Er: $R_c=8.39$ fm, $a_c=0.487$).

Nucleus	λ_f	W_V (MeV)	r_V (fm)	a_V (fm)	W_S (MeV)	r_S (fm)	a_S (fm)
^{108}Pd	1.296	19.40	1.374	0.484	1.19	1.652	0.507
^{168}Er	0.918	13.38	1.585	0.484	. . .	. . .	. . .

Since the experimental differential cross section of the $4^+_{\gamma\gamma}$ level has rather large errors, the fit of the data is only weakly influenced by this cross section. In this sense the calculated cross section is basically a prediction within the ARM.

C. The ^{108}Pd(α,α') reaction

The medium weight nuclei around $A=100$ are well known to have an almost spherical shape. Proton scattering experiments [41–43] and Coulomb excitation measurements [44] confirm the vibrational character of the low-lying natural parity states in ^{108}Pd. In a recent α-scattering experiment Riech *et al.* [13] obtained differential cross sections for the lowest $0^+,2^+,3^-$, and 4^+ states with good energy resolution at $E_\alpha=30.5$ MeV. In the analysis of these data we will show that also for the excitation of two-phonon states the folding potential as diagonal potential is adequate. First we fitted the data in the pure harmonic vibrator model coupling the 0^+_1-2^+_1-2^+_2-4^+_1-0^+_2 states where the members of the triplet are assumed to be pure two-phonon states. As a result we obtained a good description of the cross sections of the ground state and the 2^+_1 state, but the cross section of the 2^+_2 state was underestimated in the whole angular range by a factor of 2–5. On the other hand, it is known from the literature [45] that there is a direct transition from the ground state to the 2^+_2 state and that the $B(E2)$ values from the 2^+_1 to the members of the triplet are not as strong as expected from the pure HVM. So we introduced, similar to the analyses of the p scattering [41,42], a mixing between the one- and the two-phonon amplitudes for the triplet states according to Eq. (14). However, since the experiment did not allow the separation of the 0^+_2 and the 4^+_1 state, there was not enough information to fit these mixing angles. Therefore we calculated them from the ratio of existing $B(E2)$ values according to the formula

$$\varphi_I=\arcsin\sqrt{B(E2,I\rightarrow 2^+_1)/2B(E2,2^+_1\rightarrow 0^+_1)}\ , \tag{37}$$

with $I=0^+_2,2^+_2$, and 4^+_1. We want to stress that, although the ratio of the transition strengths is used as an input, the absolute values result from the fit. Additionally the strength of the one-phonon transitions is the result of an independent search and therefore the analysis predicts the $B(IS\lambda)$ values to the ground state.

In a last step we took into account the nonvanishing quadrupole moment of the 2^+_1 state. We introduced a rearrangement matrix element $\langle 2^+_1\|Q_2\|2^+_1\rangle$, which was fitted in the coupling of the 0^+_1-2^+_1-2^+_2 states. Finally the resulting matrix element was introduced in the complete coupling scheme and was kept fixed together with the mixing angles during the search of the optical model and deformation parameters. The use of the rearrangement resulted in a slightly better agreement of the cross section of the ground and the first 2^+ state.

The final results are shown in Fig. 5. The theoretical description of all transitions, except the sum of 4^+_1 and 0^+_2, is very satisfactory. The obtained optical model parameters are listed in Table III. The integral values (Table V) fit very nicely in the systematics known from lighter nuclei at comparable energies [4]. Table IV gives the deformation parameters. The mixing angles are $\varphi_{2^+_2}=60°$, $\varphi_{4^+_1}=70°$, $\varphi_{0^+_2}=-40°$ and the fitted rearrangement matrix element is $\langle 2^+_1\|Q_2\|2^+_1\rangle=1.038$. The $B(IS2)$ values are listed in Table VIII together with results from electromagnetic measurements. There is an outstanding agreement, except the $2^+_2\rightarrow 0^+_1$ transition probability, which is lower by a factor of 2. Even the quadrupole moment $Q_{2^+_1}$ coincides nicely with a recalculated value from electron scattering [46]. In the case of the $\lambda=4$ transition from the g.s. to the 4^+_1 state no value from electromagnetic measurements is known. Riech *et al.* [43] give a value of $4.7\times10^4 e^2\,\mathrm{fm}^8$ from (p,p') scattering. Similar to the observations from the ^{168}Er(α,α') reaction our value is much lower.

TABLE IV. Deformation parameters for ^{108}Pd and ^{168}Er.

Nucleus	Deformation parameters				
^{108}Pd	β_2	β_3	β'_0	β'_2	β'_4
	0.235	0.126	0.004	0.037	0.051
^{168}Er	β_2	γ_1	β_4	γ_2	γ_3
	0.216	10.3°	−0.029	−44.8°	16.1°
	β_6	γ_4	β_8		
	−0.00967	−24.9°	0.00549		

TABLE V. Band-mixing coefficients A^n_{IK} for the nth 2^+ and 4^+ levels in ^{168}Er resulting from the ARM.

	$K=0$	$K=2$	$K=4$
A^1_{2K}	0.99997	0.00812	...
A^2_{2K}	0.00812	−0.99997	...
A^1_{4K}	0.99951	0.03138	0.00009
A^2_{4K}	0.03139	−0.99950	−0.00413
A^3_{4K}	0.00003	−0.00419	0.99999

IV. SUMMARY

The aim of the present investigation was to show that the excitation of collective states by means of inelastic scattering of α particles can be well described with the use of double-folded optical potentials, calculated from mass distributions deduced from experimental charge distributions and a density-dependent effective nucleon-nucleon interaction, and that the extracted isoscalar transition probabilities compare favorably with results from electromagnetic probes. To this end the inelastic scattering of α particles on three nuclei representing completely different limiting cases of nuclear structure models has been studied.

The excitation of the first excited state of the doubly magic nucleus ^{208}Pb, the 3^- state at 2.62 MeV excitation energy, has been reanalyzed at four different incident energies. It has turned out that this highly collective state (exhausting 17% of the strength given by the energy weighted sum rule) can only be consistently reproduced if the transition potential is taken to be of the form given by the hydrodynamical model. In a recent investigation [47] of the energy dependence of pion inelastic scattering from ^{208}Pb, the same behavior is shown: energy-independent neutron and proton matrix elements for the first 3^- state can be obtained only if the HDM is used. The extracted $B(IS3,3^-\rightarrow 0^+)$ value of $0.093e^2b^3$ compares well with the result from inelastic electron scattering. At the level of precision reached in this investigation no indication for differences in the proton and neutron moments can be found in ^{208}Pb. The inelastic scattering near the Coulomb barrier can be very well reproduced using this transition potential and a Coulomb radius parameter r_C in connection with a charge density deformation parameter β_C from which again a $B(E3)$ value very close to the adopted value can be extracted. An investigation on the use of this transition potential for the inelastic α scattering on other magic nuclei is in preparation.

The nucleus ^{168}Er was investigated as an example for a good rotor. To describe not only the inelastic excitation of the ground-state band, but also that of the γ band and the bandhead of the two quadrupole phonon $\gamma\gamma$ band, the model of the asymmetric rotor was used. In this way many reduced quadrupole transition probabilities and moments could be extracted and compared to recent extensive Coulomb excitation work [39]. The value of the asymmetry angle γ, obtained from the fit, does not reproduce the energy ratio of the 2^+_γ bandhead to the first excited 2^+ of the g.s. band and represents thus only an effective γ degree of freedom. This is due to the fact that ^{168}Er is not a triaxial rotor, but a well-deformed nucleus, showing a collective γ vibration and even a two quadrupole phonon excitation, leading to the $4^+_{\gamma\gamma}$ bandhead at

TABLE VI. Volume integrals and rms radii for the optical potentials of ^{108}Pd and ^{168}Er.

Nucleus	$J_R/4A$ (MeV fm^3)	$\langle r_R^2\rangle^{1/2}$ (fm)	$J_I/4A$ (MeV fm^3)	$\langle r_I^2\rangle^{1/2}$ (fm)
^{108}Pd	346.6	5.27	59.9	5.62
^{168}Er	243.3	5.95	57.4	7.01

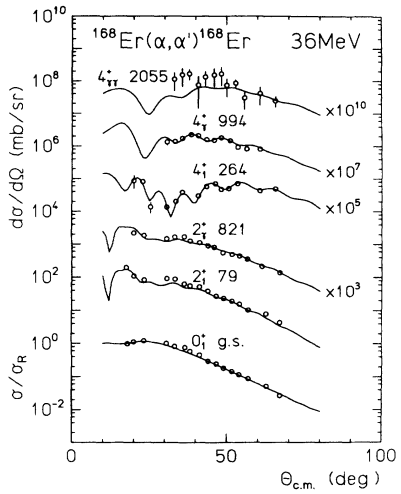

FIG. 4. Inelastic α scattering on ^{168}Er at 36 MeV. The experimental data are taken from Govil *et al.* [14]. The solid lines give the result of the analysis performed within the ARM.

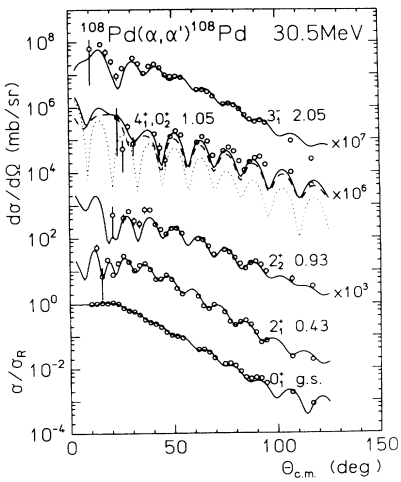

FIG. 5. Inelastic α scattering on ^{108}Pd at 30.5 MeV. The experimental data are taken from Riech *et al.* [13]. The solid lines give the result of the analysis performed in the HVM. The dotted (dashed) line gives the differential cross section of the 0^+_2 (4^+_1) state.

2055 keV excitation energy. Again the agreement between isoscalar and electromagnetic transition strength is very good.

The results can be used to independently deduce the decay properties of the 4^+ double γ vibration in ^{168}Er. The $B(IS2,4^+_{\gamma\gamma}\rightarrow 2^+_\gamma)$ value of $315e^2\,\mathrm{fm}^4$ compares very well with the result of $120e^2\,\mathrm{fm}^4 < B(E2,4^+_{\gamma\gamma}\rightarrow 2^+_\gamma) < 410e^2\,\mathrm{fm}^4$ obtained from a lifetime measurement of this level. The low hexadecapole transition probabilities found in this investigation for ^{168}Er are not in disagreement with results of Coulomb excitation experiments and point to a reduced importance of this degree of freedom in ^{168}Er.

The low-lying states in the even-even Pd nuclei are considered as good examples for vibrational modes in nuclei, therefore the nucleus ^{108}Pd was treated as a vibrator and the standard Bohr-Mottelson prescription was used for the transition potential. The energy splitting and the decay characteristics of the two-phonon triplet show the necessity to account for small anharmonicities in the description of these states. This was accomplished in representing the members of the two-phonon triplet as a

TABLE VII. Isoscalar transition probabilities $B(IS\lambda)$ for ^{168}Er obtained from inelastic α scattering compared to results from Coulomb excitation.

λ	$I_i\rightarrow I_f$	$B(IS\lambda)$[a] ($e^2\,\mathrm{fm}^{2\lambda}$)	$B(E\lambda)$[b] ($e^2\,\mathrm{fm}^{2\lambda}$)
In-band transitions ground-state band			
2	$2_1\rightarrow 0_1$	9 220	11 800(700)
2	$4_1\rightarrow 2_1$	13 200	17 100(1000)
2	$6_1\rightarrow 4_1$	14 600	22 800(1300)
2	$8_1\rightarrow 6_1$	15 400	19 700(1200)
In-band transitions γ band			
2	$4_2\rightarrow 2_2$	5 460	9 220(580)
2	$6_2\rightarrow 4_2$	10 600	15 200(900)
γ to ground transitions			
2	$2_2\rightarrow 0_1$	210	230(10)
2	$2_2\rightarrow 2_1$	410	440(40)
2	$2_2\rightarrow 4_1$	40	24(2)
2	$4_2\rightarrow 2_1$	80	110(10)
2	$4_2\rightarrow 4_1$	500	580(30)
2	$4_2\rightarrow 6_1$	30	49(23)
2	$6_2\rightarrow 4_1$	10	48(3)
2	$6_2\rightarrow 6_1$	740	420(50)
2	$6_2\rightarrow 8_1$	30	110(70)
Two-phonon to ground transitions			
2	$4_3\rightarrow 2_1$	0.01	
2	$4_3\rightarrow 4_1$	0.03	
Two-phonon to γ transitions			
2	$4_3\rightarrow 2_2$	320	
2	$4_3\rightarrow 4_2$	80	
Hexadecapole transitions to ground state			
4	$4_1\rightarrow 0_1$	11 800	
4	$4_2\rightarrow 0_1$	446 000	
4	$4_3\rightarrow 0_1$	11 200	
	$I_i\rightarrow I_f$	Q_2[a] ($e\,\mathrm{fm}^2$)	Q_2[b] ($e\,\mathrm{fm}^2$)
Quadrupole moments ground-state band			
	$2_1\rightarrow 2_1$	−190	−250(20)
	$4_1\rightarrow 4_1$	−240	−240(30)
Quadrupole moments γ band			
	$2_2\rightarrow 2_2$	190	216(7)
	$4_2\rightarrow 4_2$	−100	−140(10)
Quadrupole moment two-phonon band			
	$4_3\rightarrow 4_3$	350	

[a]This work.
[b]Reference [39].

TABLE VIII. Isoscalar transition probabilities $B(IS\lambda)$ for ^{108}Pd obtained from inelastic α scattering compared to results from e.m. probes.

λ	$I_i \rightarrow I_f$	$B(IS\lambda)$[a] ($e^2\,\mathrm{fm}^{2\lambda}$)	$B(E\lambda)$[b] ($e^2\,\mathrm{fm}^{2\lambda}$)
2	$2_1 \rightarrow 0_1$	1 630	1 560(40)
2	$2_2 \rightarrow 0_1$	10	25(3)
2	$2_2 \rightarrow 2_1$	2 440	2 380(210)
2	$4_1 \rightarrow 2_1$	2 870	2 810(370)
2	$0_2 \rightarrow 2_1$	1 340	1 340(300)
3	$3_1 \rightarrow 0_1$	16 300	14 900(4300)[c]
4	$4_1 \rightarrow 0_1$	12 800	
	$I_i \rightarrow I_f$	Q_2[a] ($e\,\mathrm{fm}^2$)	Q_2[d] ($e\,\mathrm{fm}^2$)
	$2_1 \rightarrow 2_1$	−71	−70(27)

[a]This work.
[b]Reference [45].
[c]Reference [32].
[d]Reference [46].

mixture of two-phonon and one-phonon states. The mixing was fixed by the known ratio of the $B(E2)$ values from the triplet states to the one-phonon 2^+ state and from this state to the ground state. The resulting reduced $B(IS\lambda)$ values and the quadrupole moment correspond extremely well with the results from electromagnetic probes.

The excellent agreement of the isoscalar transition probabilities obtained from the present analysis of inelastic α-scattering data on three different nuclei with results from other experiments shows that reliable values can be extracted using the method outlined in this work and indicates that this method allows us to also obtain transition probabilities for higher multipolarities unaccessible with electromagnetic probes.

ACKNOWLEDGMENTS

We would like to thank Professor G. Staudt and his collaborators for many enlightening discussions. We also are greatly indebted to Dr. V. Riech for the communication of the ^{108}Pd(α,α') data prior to publication and the permission to use them in this work. This work has been funded by the German Federal Minister for Research and Technology at Bundesministerium für Forschung und Technologie (BMFT) under Contract No. 06 Tü460.

[1] A. M. Bernstein, Adv. Nucl. Phys. **3**, 325 (1969).
[2] G. R. Satchler, J. Math. Phys. **13**, 1118 (1972).
[3] H. Abele, H. J. Hauser, A. Körber, W. Leitner, R. Neu, H. Plappert, T. Rohwer, G. Staudt, M. Strasser, S. Welte, M. Walz, P. D. Eversheim, and F. Hinterberger, Z. Phys. A **326**, 373 (1987).
[4] R. Neu, S. Welte, H. Clement, H. J. Hauser, G. Staudt, and H. Müther, Phys. Rev. C **39**, 2145 (1989).
[5] J. Fritze, R. Neu, H. Abele, F. Hoyler, G. Staudt, P. D. Eversheim, F. Hinterberger, and H. Müther, Phys. Rev. C **43**, 2307 (1991).
[6] K. P. Kocher, R. Neu, F. Hoyler, H. Abele, P. Mohr, G. Staudt, P. D. Eversheim, and F. Hinterberger, Phys. Rev. C **45**, 123 (1992).
[7] H. de Vries, C. W. de Jager, and C. de Vries, At. Data Nucl. Data Tables **36**, 495 (1987).
[8] A. M. Kobos, B. A. Brown, R. Lindsay, and G. R. Satchler, Nucl. Phys. **A425**, 205 (1984).
[9] J. S. Lilley, M. A. Franey, and Da Hsuan Feng, Nucl. Phys. **A342**, 165 (1980).
[10] L. L. Rutlege, Jr., and J. C. Hiebert, Phys. Rev. C **13**, 1072 (1976).
[11] V. Corcalciuc, H. Rebel, R. Pesl, and H. J. Gils, J. Phys. G **9**, 177 (1983).
[12] D. A. Goldberg, S. M. Smith, H. G. Pugh, P. G. Roos, and N. S. Wall, Phys. Rev. C **7**, 1938 (1973).
[13] V. Riech, R. Scherwinski, G. Lindström, E. Fretwurst, K. Gridnev, P. P. Zarubin, and R. Kolalis (unpublished).
[14] I. M. Govil, H. W. Fulbright, D. Cline, E. Wesolowski, B. Kotlinski, A. Baklin, and K. Gridnev, Phys. Rev. C **33**, 793 (1986).
[15] H. G. Börner, J. Jolie, S. J. Robinson, B. Krusche, R. Piepenbring, R. F. Casten, A. Aprahamian, and J. P. Draayer, Phys. Rev. Lett. **66**, 691 (1991).
[16] See, for example, N. Yoshinaga, Y. Akiyama, and A. Arima, Phys. Rev. C **38**, 419 (1988); S. Kuyucak and I. Morrison, Ann. Phys. (N.Y.) **181**, 79 (1988).
[17] G. J. Horowitz and B. D. Serot, Nucl. Phys. **A368**, 503 (1981).
[18] G. R. Satchler and W. G. Love, Phys. Rep. **55**, 183 (1979).
[19] T. Tamura, Rev. Mod. Phys. **37**, 679 (1965).
[20] L. J. Tassie, Aust. J. Phys. **9**, 407 (1956).
[21] T. Tamura, Prog. Theor. Phys. (Suppl.) **37/38**, 383 (1966).
[22] A. S. Davydov and G. F. Filippov, Nucl. Phys. **8**, 237 (1958).
[23] F. T. Baker, Nucl. Phys. **A331**, 39 (1979).
[24] H. Rebel, G. Hauser, G. W. Schweimer, G. Nowicki, W. Wiesner, and D. Hartmann, Nucl. Phys. **A218**, 13 (1974).
[25] R. S. Mackintosh, Nucl. Phys. **A266**, 379 (1976).
[26] H. Rebel, Z. Phys. A **277**, 35 (1976).
[27] D. K. Srivastava and H. Rebel, Z. Phys. A **316**, 225 (1984).
[28] H. Clement, G. Graw, H. Kader, F. Merz, H. J. Scheerer, P. Schiemenz, and N. Seichert, Nucl. Phys. **A451**, 219 (1986).
[29] D. K. Srivastava and H. Rebel, J. Phys. G **10**, L127 (1984).
[30] M. El-Azab Farid and G. R. Satchler, Nucl. Phys. **A481**, 542 (1988).
[31] J. Raynal, computer code ECIS (unpublished).
[32] R. H. Spear, At. Data Nucl. Data Tables **42**, 55 (1989).
[33] F. E. Bertrand, G. R. Satchler, D. J. Horen, J. R. Wu, A. D. Bacher, G. T. Emery, W. P. Jones, D. W. Miller, and A. van der Woude, Phys. Rev. C **22**, 1832 (1980).

[34] H. Abele, K. Kocher, R. Neu, and G. Staudt, Verhandl. DPG(VI) **25**, PA8 (1990); H. Abele (private communication).
[35] S. Raman, At. Data Nucl. Data Tables **36**, 1 (1987).
[36] P. Raghavan, At. Data Nucl. Data Tables **42**, 189 (1989).
[37] W. F. Davidson, D. D. Warner, R. F. Casten, K. Schreckenbach, H. G. Börner, J. Simic, M. Stoyanovic, M. Bogdanovic, S. Koicki, W. Gelletly, G. B. Orr, and M. L. Stelts, J. Phys. G 7, 455 (1981).
[38] R. Piepenbring and M. K. Jammari, Nucl. Phys. **A481**, 81 (1988).
[39] B. Kotliński, D. Cline, A. Bäcklin, K. G. Helmer, A. E. Kavka, W. J. Kernan, R. M. Diamond, A. O. Macchiavelli, and M. A. Deleplanque, Nucl. Phys. **A517**, 365 (1990).
[40] T. Ichihara, H. Sakaguchi, M. Nakamura, M. Yosoi, M. Ieiri, Y. Takeuchi, H. Togawa, T. Tsutsumi, and S. Kobayashi, Phys. Rev. C **36**, 1754 (1987).
[41] R. L. Robinson, J. L. C. Ford, Jr., P. H. Stelson, and G. R. Satchler, Phys. Rev. **146**, 816 (1966).
[42] K. Koike, T. Suehiro, K. Pingel, K. Komura, I. Nonaka, T. Wada, T. Fujisawa, H. Kamitsubo, and T. Nojiri, Nucl. Phys. **A248**, 237 (1975).
[43] V. Riech, E. Fretwurst, G. Lindström, K. F. von Reden, R. Scherwinski, and H. P. Blok, Phys. Lett. B **178**, 10 (1986).
[44] I. Y. Lee, N. R. Johnson, F. K. McGowan, R. L. Robinson, M. W. Guidry, L. L. Riedinger, and S. W. Yates, Phys. Rev. C **25**, 1865 (1982).
[45] Nucl. Data Sheets **62**, 804 (1991).
[46] W. K. Koo and L. J. Tassie, J. Phys. G 7, L63 (1981).
[47] D. S. Oakley, R. J. Peterson, S. J. Seestrom, C. L. Morris, M. A. Plum, J. D. Zumbro, A. L. Williams, M. A. Bryan, J. W. McDonald, and C. Fred Moore, Phys. Rev. C **44**, 2058 (1991).